



ELSEVIER

Available online at www.sciencedirect.com



Nuclear Physics B (Proc. Suppl.) 175–176 (2008) 551–554

NUCLEAR PHYSICS B
PROCEEDINGS
SUPPLEMENTS

www.elsevierphysics.com

Preliminary results of the Moon shadow using ARGO-YBJ detector

Yungang Wang^a*, on behalf of the ARGO-YBJ Collaboration[†].

^aInstitute of High Energy Physics, Chinese Academy of Sciences 19B Yuquan Lu, Shijingshan, Beijing, 100049, P.R.China

ARGO-YBJ is a "full coverage" air shower detector consisting of Resistive Plate Chambers (RPCs) at the Yangbajing High Altitude Cosmic Ray Laboratory (Tibet, China) at 4300 m a.s.l. (lat=30.11° N, long=90.53° E). Using the data collected with a carpet of RPCs (1900 m², about 1/3 of the whole ARGO-YBJ detector), the cosmic ray shadowing effect due to the Moon was studied. The 50% angular resolution is found to be $\sim 1.2^\circ$ with the Chess-board method and the Moon shadow with a significance of 4.9σ is found displaced by 0.7° westward and 0.5° northward with respect to the expected position by the equi-zenith angle Method.

1. Introduction

It was originally suggested by Clark[1] in 1957 that the interception of the cosmic ray by the Moon (Sun) will lead to event deficit from the direction of the Moon (Sun), and this shadowing effect is usually known as the Moon (Sun) shadow of the cosmic ray. However, the Moon (Sun) shadow hasn't been observed until two crucial criteria were fulfilled many years later. The first condition is that the cosmic ray should be insensitive or only weakly sensitive to the geomagnetic field; the second requires that the detector has to have a good angular resolution[2]. The first successful observation of the Moon shadow was made by CYGNUS collaboration in 1992[3]. Later on, experiments such as CASA, TIBET-AS γ , MACRO, L3+c, MILAGRO have also observed the cosmic ray Moon Shadow.

The observation of the Moon shadow is important for ground-based detectors. The spread and the shape of the Moon shadow is governed by the angular resolution and by possible pointing biases of the detector. Through the Moon shadow, the \bar{p} content in the cosmic ray flux can be studied[4]. The use of the Moon collimation allows a rough charge identification in the Earth magnetic field. Negatively charged primaries in cosmic rays

are deflected towards the west, while positively charged primaries towards the east. If antiprotons are present in the cosmic ray flux, they will generate a shadow on the opposite side of the Moon relative to the shadow from dominant cosmic rays induced from matter. The observation of the Moon shadow can also be used to perform absolute energy calibration for ground-based AS array[5].

2. ARGO-YBJ array

The ARGO-YBJ detector consists of a single layer RPCs and is logically divided into 154 units called Clusters (7.64 \times 5.72 m²), each made up of 12 RPC operated in streamer mode with a mixture of argon (15%), isobutane (10%) and tetrafluoroethane (75%). The detector is composed of the central continuous carpet (130 clusters) and the guard ring (24 clusters). Each RPC (1.26 \times 2.85 m²) is read out with 10 pads (62 \times 56 cm²), which are further divided into 8 different strips (62 \times 6.7 cm²) providing the high available space resolution. The whole system is designed to provide a single hit (pad) time resolution at the level of 1 ns, allowing a complete and detailed three dimensions reconstruction of the shower front. In order to convert a fraction of the secondary gamma rays into charged particles, and reduce the time spread of the shower front and increase the angular resolution, the detectors will be covered by a 0.5 cm thick layer of lead[6].

*E-mail address: wangyg@mail.ihep.ac.cn

[†]This work is supported partly by the Chinese Academy of Sciences, the Ministry of Science and Technology and the National Science Foundation of China.

Since December 2004, a carpet of 42 Clusters(ARGO-42, $47 \times 41 m^2$) has been operated without lead converter sheet. In this analysis, the data collected from December 2004 to April 2005 with ARGO-42 have been used.

3. Angular resolution estimate

The angular resolution of the carpet is estimated by the Chess-board method[6]. In this method, the overall detector is divided into two independent sub-arrays, one is made of the "odd" pads and the other is made of the "even" pads. Where "odd" and "even" refers to contiguous elements out of a unique numbering method of all the pads in the detector. The two sub-arrays overlap spatially so that they sample the same portion of the shower. The direction of one event can be reconstructed with the even array and the odd array respectively. The opening angle $M_{\Delta\theta}$ is a measurement of the angular spread between the two estimates, which contains 50% of the reconstructed events. The 50% angular resolution θ_{50} can be estimated as $\theta_{50} = M_{\Delta\theta}/2$ [6]. In this

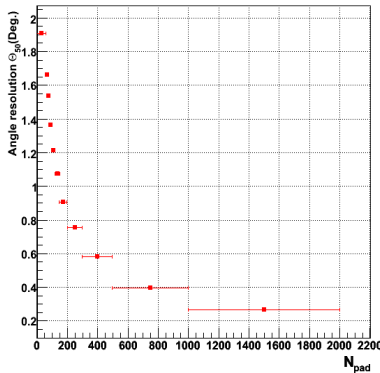


Figure 1. The θ_{50} as a function of the number of fired pads for ARGO-42 with the Chess-board method

analysis, the shower direction is reconstructed by means of an iterative procedure, assuming the shower front is in a conical structure, with a cone slope of 0.03 [7] fixed for all events. The relative time offsets among different pads have been calibrated with the method described in[8]. For

the purpose of angular resolution analysis, the reconstructed events are further selected by imposing the following cuts: a) being an internal event (event with core inside the detector) ; b) zenith angle $\leq 40^\circ$; c) $(\chi^2/nhit) < 1$ (here, χ^2 is the summation of the weighted residual square running over the pads used in the directional reconstruction and nhit is the corresponding number of pad). After these cuts, the value obtained for θ_{50} as a function of the number of fired pads for ARGO-42 is shown in Fig.1. On the average, θ_{50} is $\sim 1.2^\circ$ for all selected events without considering the number of fired pads.

4. Experiment data analysis

In this work, the equi-zenith angle Method is used to estimate the background in order to extract the deficit signal of cosmic-ray events from the Moon direction. In practice, the number of background events is obtained by averaging the number of events from 6 off-source space-time windows which have the same shape and are in same time interval as the on-source window, at the same zenith angle. This method can eliminate the systematic effects caused by environmental parameters such as atmospheric pressure and temperature fluctuations. In this analysis, 6.45×10^8 events were reconstructed from the raw data collected in 1263 running hours. The events are selected by the same cuts used in above mentioned angular resolution analysis and 2.1×10^8 events remain. The significance of the deficit shadow is calculated as $S = (N_{on} - N_{off}) / \sqrt{N_{on} + \varepsilon N_{off}}$, $\varepsilon = 1/6$. Here, N_{on}/N_{off} stand for the total number of events which are in a circle in on/off source window. To optimize the sensitivity[9], the radius(smoothing radius) of the circle is chosen to be 1.5° . Figure 2 shows the significance map of Moon shadow from ARGO-42 data. A peak of 4.9σ in the significance map is located at 0.7° towards the west and 0.5° towards the north with respect to the expected Moon position. Figure.3 shows the significance distribution for on source window over sampled on a grid of 0.2° by 0.2° . The longer tail in negative side indicates the event deficit due to Moon shadowing.

The incremental number of deficit events as a

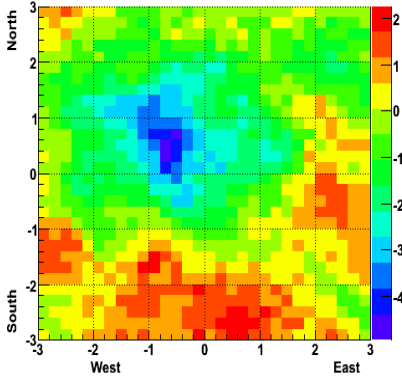


Figure 2. The significance map of Moon shadow from ARGO-42 data: A peak of 4.9σ is located at 0.7° towards the west and 0.5° towards the north with respect to the expected position by 1.5° smoothing radius.

function of Modified Julian Date(MJD) is made for the direction which has the lowest significance value in Fig.2. When the angular resolution is described by a Gaussian distribution, with θ_{50} a few times larger than the apparent Moon size, the number of deficit events can be estimated by the following formula[9]:

$$N_{deficit} \sim \eta \times N_{moon} \quad (1)$$

$$\eta = 1 - e^{-0.5 \times (\frac{R_{smooth}}{\theta_{50}/1.177})^2} \quad (2)$$

where N_{moon} is the number of all deficit events shadowed by the Moon, R_{smooth} is the radius of smoothing window, θ_{50} is the angular distance, measured from the original event direction, which contains 50% of the events. The distribution of the expected deficit events with $\theta_{50} = 1.2^\circ$ and in $R_{smooth} = 1.5^\circ$ is shown in Fig.4. The distribution agree very well between observation and expectation.

5. Monte Carlo simulation

A full MC simulation procedure is firstly adopted to generate the "missing" events sample which served as a negative imaging of the Moon shadow. In this calculation, we choose the IGRF model[10] to describe the geomagnetic field for altitude smaller than 600 km and the dipole

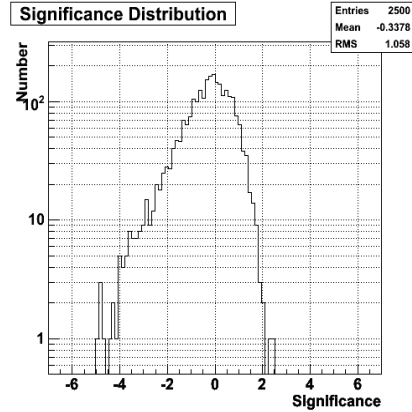


Figure 3. The significance distribution for on source window over sampled on a grid of 0.2° by

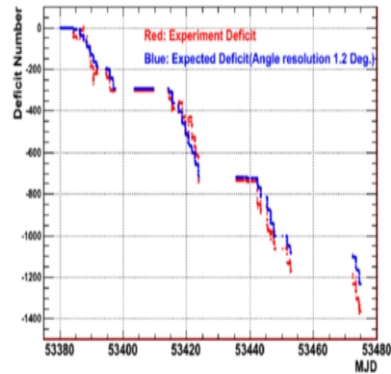


Figure 4. The distribution of expected deficit as a function of MJD

model ($8.07 \times 10^{25} G \cdot cm^3$) for altitude above 600 km. The CORSIKA6200(QGSJET)[11] is used to perform the air shower simulation. We adopt a primary cosmic rays flux based on direct observational data[12–14] with the primary energy ranging from 0.1 TeV to 1000 TeV. The MC events are generated on top of the atmosphere randomly along the Moon’s orbit within a window of size $\pm 10^\circ \times \pm 10^\circ$ centered at the Moon. Then, we reverse the charge of each event and have it shot back toward the Moon including the deflexion effect which comes from the geomagnetic field. Those which hit the Moon are collected as the “missing events” and are used for the detailed detector simulation via a package based

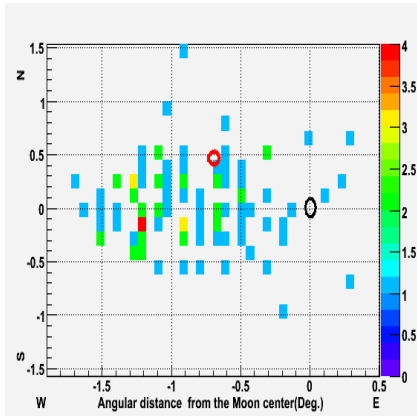


Figure 5. The distribution of shadow center. The black circle is the center of Moon and the red circle is the Moon shadow center from experiment data. The color scale indicates the number of toy MC experiments.

on GEANT-3. After the simulation, the angular distribution of “missing events” can be obtained including the effect of cascading in the atmosphere and interaction in ARGO detector. To save CPU time, the angular distribution of background events is directly taken from the observation. Based on the angular distribution of “missing events” and background events, 100 toy MC experiments are generated to study the position and significance of the Moon shadow. The distribution of shadow center is shown in Fig.5 and the significance of the deficit is shown in Fig.6. Both the position and the significance of moon shadow from ARGO-42 data are in good agreement with the MC expectation.

6. Summary

ARGO-42 data taken from December 2004 to April 2005 have been reconstructed and used to analyze the Moon shadow. With the Chess-board method, the 50% angular resolution has been estimated to be $\sim 1.2^\circ$. The estimate shows to be consistent with the number of missing events obtained from Moon shadow analysis. With this set of data sample, the Moon shadow with a significance of 4.9σ is found with an offset, with respect to the expected position, of 0.7° westward

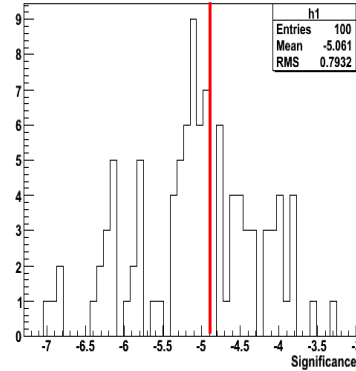


Figure 6. The significance distribution of Moon shadow. The red line is the significance of Moon shadow from experiment data.

and 0.5° northward. This preliminary result is in agreement with the MC expectation.

REFERENCES

1. G.W. Clark, Phys.Rev. 108(1957)450.
2. P.Achard et al. L3 Collaboration, AstroPhy 23 (2005) 411-434
3. D.E Alexandreas et al. CYGNUS Collaboration, Phys.Rev.D 43 (1991) 1735.
4. M.Urban et al., Nucl. Phys. B(Proc. Suppl.), 14B(1990) 233.
5. M.Amenomori et al. the Tibet AS γ Collaboration, 29th ICRC Pune(2005)00,101-106
6. C. Bacci et al. ARGO-YBJ Collaboration, Astropart. Phys. 17 (2002) 151-165
7. G. Di Sciasci et al., 29th ICRC, Pune6, 33(2005)
8. P.Bernardini et al., 29th ICRC, Pune5, 147(2005)
9. CHEN Xin et al. Hep&Np Vol.28, No.10 (2004)
10. National Geophysical Data Center web site
11. D.Heck et al., Report FZKA, 6019, Forschungszentrum Karlsruhe (1998)
12. Asakimori,k., et al. 1998, ApJ, 502,278
13. Kamioka,E., et al. 2001, Adv.Space Res., 26.1839
14. Sanuki,T., et al. 2002, ApJ, 545,1135